Synthesis of Biodegradable and Electroactive Multiblock Polylactide and Aniline Pentamer Copolymer for Tissue Engineering Applications

Lihong Huang,[†,‡] Xiuli Zhuang,[†] Jun Hu,[†,‡] Le Lang,[†,‡] Peibiao Zhang,[†] Yu Wang,[†] Xuesi Chen,[*,†] Yen Wei,[*,§] and Xiabin Jing[†]

State Key Laboratory of Polymer Physics and Chemistry, Changchun Institute of Applied Chemistry, Chinese Academy of Sciences, Changchun 130022, China, Graduate School of Chinese Academy of Sciences, Beijing 100039, China, and Department of Chemistry and School of Biomedical Engineering, Drexel University, Philadelphia, Pennsylvania 19104

Received October 25, 2007; Revised Manuscript Received January 8, 2008

To obtain one biodegradable and electroactive polymer as the scaffold for tissue engineering, the multiblock copolymer PLAAP was designed and synthesized with the condensation polymerization of hydroxyl-capped poly(L-lactide) (PLA) and carboxyl-capped aniline pentamer (AP). The PLAAP copolymer exhibited excellent electroactivity, solubility, and biodegradability. At the same time, as one scaffold material, PLAAP copolymer possesses certain mechanical properties with the tensile strength of 3 MPa, tensile Young 's modulus of 32 MPa, and breaking elongation rate of 95%. We systematically studied the compatibility of PLAAP copolymer in vitro and proved that the electroactive PLAAP copolymer was innocuous, biocompatible, and helpful for the adhesion and proliferation of rat C6 cells. Moreover, the PLAAP copolymer stimulated by electrical signals was demonstrated as accelerating the differentiation of rat neuronal pheochromocytoma PC-12 cells. This biodegradable and electroactive PLAAP copolymer thus possessed the properties in favor of the long-time application in vivo as nerve repair scaffold materials in tissue engineering.

1. Introduction

Because of the crucial replacement and restoration of biological function, polymeric scaffold materials have been widely studied and applied in tissue engineering.[1–3] In the past few decades, a great deal of natural biopolymers and synthetic polymers, such as collagen,[4] chitosan (CS),[5,6] polylactide (PLA),[7–9] poly (ϵ-caprolactone) (PCL),[10] and their composites[11–14] have been used as the tissue engineering scaffold materials because they are of good biocompatibility, biodegradability, and specific tissue-using mechanical properties. Nowadays, the demand of current clinical treatment has developed more novel biomaterials with specific target functions, externally controlled or tailored by surrounding stimulation, including light,[15] electrical signal,[16] magnetic power,[17] and the change of pH.[18]

One important field of tissue engineering is the application to repair peripheral nerve damage. A number of different classes of materials have been investigated as potential nerve guidance channels to bridge the gap between severed nerve ends instead of the autologous nerve graft because the autografts have several drawbacks, including the need for multiple surgical procedures and loss of function at the donor site.[19] Stimulus-responsive polymers show great promise as new "smart" biomaterials. The electroactive polymer, being electrical stimulus responsive, has become the focus of research because electrical charges were proved to play an important role in stimulating either the proliferation or differentiation of various cell types.[20–22]

Nowadays, one kind of the electroactive polymers, the electrically conductive polymer such as polypyrrole (PPy) and polyaniline (PANi), have been the most thoroughly investigated for use in biological systems due to the key advantage of permitting external control over the intensity and duration of stimulation. Electrically conducting polymers characteristically have a conjugated backbone with a high degree of w-orbital overlap. Through a process "doping−dedoping", the neutral polymer chain can become either positively charged or negatively charged, respectively, with polarons and bipolarons as the charge carriers for electrical conduction.[23,24] This doping process is reversible and can be achieved either chemically or electrochemically. When an electrical stimulation is applied on the electrically conducting polymers, the dopant distributes in and out the polymer with the switch of polymer between the conductive and insulating states,[25] and the changes of polymer surface properties, including charge density, wettability, conformational, and dimensional changes can influence the growth and proliferation of cells.[26,27]

The conducting polymers, especially PPy, have been found to be widely studied in biomedical applications. Schmidt et al. have made great contribution to the application of electrically conducting PPy in the biomedical field.[28–30] They first employed PPy for tissue engineering purposes, demonstrating that an electrical stimulus in NGF-induced PC-12 cells cultured on PPy significantly enhanced PC-12 neurite outgrowth and spreading. Moreover, they further studied the reason why PPy could enhance the cell extension and concluded that the electrical stimulation increases the adsorption of serum proteins, which help to improve the growth and proliferation of cells. Subsequently, Lakard et al.,[31] George et al.,[32] and several other groups investigated cell adhesion and proliferation cultured different cell lines on PPy.[33–35]

* Corresponding authors. E-mail: xschen@ciac.jl.cn. Telephone: +86-431-85262112. Fax: +86-431-85685653 (X.C.); E-mail: weiyen@drexel.edu. Telephone: (215)895-2650. Fax: (215)895-1265 (Y.W.).
† Changchun Institute of Applied Chemistry.
‡ Graduate School of Chinese Academy of Sciences.
§ Drexel University.

10.1021/bm7011828 CCC: $40.75
Published on Web 02/09/2008

By comparison, few considerations have been paid to PANi, one of the best conducting polymers, as potential conductive substrates for tissue engineering application. Mattioli-Belmonte et al. first demonstrated that PANi was biocompatible in vitro and in long-term animal studies in vivo.[36] In recent years, Wei et al. reported that PANi films functionalized with the bioactive laminin-derived adhesion peptide YIGSR (Tyr-Ile-Gly Ser-Arg) exhibited significant enhanced PC-12 cell attachment and differentiation.[37,38] In studying the influence of the surface conductivity of the emeraldine salt form of PANi on H9c2 rat cardiac myoblast cells, they determined that adhesion to and proliferation on unmodified electrical conductive PANi surfaces were essentially the same as that on tissue-culture-treated polystyrene (TCPS).[39] More recently, they demonstrated the biocompatibility of electrospun nanofibers containing camphorsulfonic acid-doped PANi and gelatin, which might serve as potential scaffold materials for cardiac tissue engineering.[40] Despite a great deal of research reporting the positive influence of electrically conducting PANi to neural cells, there are some problems in practical application such as the poor solubility and processibility. However, the key limitation factor of PANi applied in biological systems is their nondegradability. Remaining the electrically conducting polymer for a long time in vivo can bring the inflammation and need the second surgery for removal. Designing and synthesizing of degradable PANi-based electroactive copolymer materials may be one promising way to realize the clinical application as nerve tissue engineering scaffold materials.

In our previous paper,[41] PLA-*b*-AP-*b*-PLA (PAP) triblock copolymer of poly(l-lactide) (PLA) and aniline pentamer (AP) was synthesized. This triblock copolymer is electroactive and biodegradable. PLA is well known for its good solubility, biocompatibility, and biodegradability. With the introduction of PLA segment, this PAP triblock copolymer showed good solubility and processibility. In vitro cell experiments proved the excellent biocompatibility of the PAP triblock copolymer. This biodegradable PAP copolymer with electroactive function would be potentially used as scaffold materials for neuronal or cardiovascular tissue engineering. However, because of the low molecular weight ($M_w < 10000$), the mechanical properties and plasticity of the PAP triblock copolymer material are not good in practical application.

To improve the material mechanical properties, recently we designed and gained one novel alternant multiblock PLAAP copolymer of poly(L-lactide) (PLA) and aniline pentamer (AP) with the condensation polymerization reaction. This PLAAP multiblock copolymer possessed excellent electroactivity, solubility, and biodegradability similar to the PAP triblock copolymer and had the better mechanical properties due to the higher molecular weight (about $M_w = 100000$), which provide more feasibility in practical application. The biological properties of PLAAP copolymer were investigated deeply. In vitro cell evaluation showed that the electroactive PLAAP copolymer was innocuous and could indeed promote the attachment and growth of rat C6 glioma cells. Moreover, the comparison experiments with and without applying an electrical potential demonstrated that PLAAP copolymer in the doping state had the ability of improving the differentiation of rat neuronal pheochromocytoma PC-12 cells, which suggests the promising application of PLAAP copolymer as nerve repair scaffolds in tissue engineering.

2. Experimental Section

Materials. *N*-phenyl-1,4-phenylenediamine, *p*-phenylenediamine, *N*,*N*′-dicyclohexyl carbodiimide (DCC), 4-dimethylaminopyridine (DMAP), 1,4-butanediol (BDO), stannous octoate [$Sn(Oct)_2$, 95%], and camphorsulfonic acid (CSA) were purchased from Aldrich. Butane diacid anhydride and ammonium persulfate were purchased from Chemical Reagent Beijing Co., Ltd. All the reagents above were used as received without further purification. L-Lactide was prepared from our group and recrystallized for three times before polymerization. *N*-Methyl-pyrrolidome (NMP), toluene, and ethyl acetate were distilled after drying with CaH_2. *N*,*N*-Dimethylformamide (DMF), tetrahydrofuran (THF), methylene chloride (CH_2Cl_2), chloroform ($CHCl_3$), ethyl ether, ethanol, 1,2-ethylene chloride, hydrochloric acid (HCl), and ammonia were used as received.

Synthesis and Characterization of the PLAAP Multiblock Copolymer. Hydroxyl-capped poly(L-lactide) (PLA) was obtained from ring-opening polymerization initiated with BDO. Carboxyl-capped aniline pentamer in emeraldine base state (EM AP) was synthesized from the oxidative coupling of *N*-phenyl-1,4-phenylenediamine protected with butane diacid anhydride and *p*-phenylenediamine with ammonium persulfate as the oxidants. The detailed synthesis methods of PLA and EM AP were described in our previous paper.[41]

To avoid the influence of the low molecular compounds such as ethanol and H_2O, PLA was azeotropically distilled in toluene for 18 h first. Then 2 mmol of purified PLA, 2 mmol of emeraldine of EM AP, 5 mmol of DCC, 5 mmol of DMAP, and 12 mL NMP were added into a flame-dried glass reactor. After being nitrogen-purged three times, the reactor was then sealed and cooled to 0 °C for 48 h with magnetic stirring.[42] After the reaction, dicyclohexylurea was removed by filtration. The copolymer in the filtrate was precipitated in ethanol and was dissolved in $CHCl_3$, followed by precipitation in ethyl ether. Such a dissolution−precipitation process was repeated three times to purify the product. The final product, emeraldine of the multiblock copolymer (EM PLAAP), was dried under vacuum at room temperature for 24 h. The synthesis of the fully reduced leucoemeraldine of the copolymer (LM PLAAP) was achieved by reducing the EM PLAAP dissolved in THF with hydrogen at 3 atm over platinum oxide for 2 h.[43] After reduction, the residual platinum oxide was removed by filtration. Under protection of nitrogen, the light-gray LM PLAAP product was obtained by precipitation with ethyl ether. The LM PLAAP copolymer was then dried under reduced pressure at room temperature for 24 h and stored with the protection of N_2 at 4 °C.

The resulting product was subsequently characterized as follows: ^{1}H nuclear magnetic resonance (NMR) spectra were recorded on a Bruker AV 400 MHz spectrometer with DMSO-d_6 as the solvent at room temperature. FT-IR spectra of the PLAAP powders were recorded on a Bio-Rad Win-IR instrument. Matrix-assisted laser desorption/ionization time-of-flight (MALDI-TOF) mass spectra were performed on an AXIMA-CFR laser desorption ionization time-of-flight spectrometer (COMPACT). Gel permeation chromatography (GPC) measurements were carried out at 35 °C with a Waters 505 GPC instrument equipped with three Waters Styragel columns (HT3, HT4, and HT5) and a differential refractometer detector. $CHCl_3$ was used as an eluent at a flow rate of 1 mL/min. The molecular weights were calibrated with polystyrene standards. The UV–visible spectra of the copolymer solutions were monitored on a UV–vis spectrophotometer (UV-2401). Samples for cyclic voltammetry were prepared by depositing thin LM PLAAP film on an indium tin oxide (ITO) electrode as working electrode and Ag/Ag^+ as the reference electrode. Cyclic voltammograms were recorded on a CHI 630 potentiostat with a scanning rate of 50 mV s^{-1}. The standard Van Der Pauw dc four-probe method was used to measure the electrical conductivity of the PLAAP copolymer film (doped with CSA). The square sample was placed on the four-probe apparatus. Providing a voltage, a corresponding electrical current could be obtained. The electrical conductivity of samples was calculated by the following formula: σ (S/cm) = (2.44 × 10/*S*) × (*I*/*E*), where σ is the conductivity, *S* is the sample side area, *I* is the current passed through outer probes, and *E* is the voltage drop across inner probe. Differential scanning calorimetry (DSC) was carried out on a TA Instrument Q100 under nitrogen atmosphere. Measurements during the

first heating from 0 to 180 °C and then the first cooling from 180 to 0 °C as well as the second heating from 0 to 180 at 10 °C /min were performed. Thermal gravimetric analysis (TGA) (TA Instrument Q500) was used to determine the ratio of PLA and AP. The measurements were performed at 5 °C /min from room temperature up to 800 °C. For the tensile strength test, the specimens of EM PLAAP were prepared as 5 mm × 10 mm × 0.2 mm. Normal tensile tests were conducted on an Instron 1121 machine at a crosshead speed of 1 mm/min. The tensile strength and modulus data were both obtained by averaging over six specimens. Water contact angles ($n = 8$) were measured by the sessile drop method on a VCA2000 contact angle instrument (AST Products).

Characterization of LM PLAAP copolymer: ^{1}H NMR (400 MHz, DMSO-d_6) δ 9.73 (s, 2H), 7.61 (s, 2H), 7.51 (s, 2H), 7.36 (d, 4H), 6.95−6.83 (m, 16H) for AP segment, and 5.17 (t, 1H, poly), 4.22 (t, 1H), 4.09 (s, 2H), 1.47 (d, 3H, poly), 1.27 (d, 3H) for PLA segments. ^{13}C NMR (100 MHz, DMSO-d_6) δ 173.95 (−CO-NH−), 171.83 (−CO-O−), 169.12 (poly −CO−), 140.87 (Ar-C), 138.33 (Ar-C), 137.11 (Ar-C), 135.57 (Ar-C), 130.58 (Ar-C), 120.44 (Ar-C), 119.53 (Ar-C), 118.33 (Ar-C), 117.47 (Ar-C), 115.29 (Ar-C), 68.64 (poly −CH−), 64.49 (−CH_2−), 30.32 (−CH_2−), 28.51(−CH_2−), 24.32 (−CH_2−), 16.41(poly −CH_3). IR (neat, cm^{-1}) 2999 (w, ν_{as} CH_3), 2946 (w, ν_{OH}), 1759 (s, $\nu_{C=O}$ for ester bond), 1672 (m, $\nu_{C=O}$ for amide bond), 1503 (s, $\nu_{C=C}$ of benzenoid rings), 1451 (s, δ_s CH_3), 1388 (w, δ_{as} CH_3), 1361 (w, δ_s C-CH_3), 1187, 1093 (m, ν_{O-C-O}), 868, 755 (s, γ C-CH_3).

Preparation of Copolymer Thin Films. The copolymer sample was dissolved in $CHCl_3$ to form 5 wt % solutions. The solutions were cast onto a superflat polytetrafluoroethylene plates and placed for 5 h under room temperature to form thin films. The films thus obtained were dried under reduced pressure at room temperature for 48 h to remove $CHCl_3$.

Degradation of Copolymers. For degradation studies, each specimen (10 mm × 10 mm × 0.2 mm) of PLAAP copolymer made from films were placed in tubes filled with 10 mL of 0.5 M Tris-HCl buffer solution (pH = 8.6) containing 0.6 mg of proteinase K. The tubes were placed in the thermostatic shaker at 37 °C. The buffer solution containing proteinase K was changed every two days. After different time, the specimens were taken out and washed with distilled water for three times, then dried at room temperature in vacuum for one week before being subjected to loss weight analysis. Three samples were prepared in each time interval. The loss weight is gained from the average value of three samples.

C6 Cell Adhesion and Proliferation. For PLA, LM PLAAP, EM PLAAP, and EM PLAAP doped with CSA, every polymer was respectively dissolved in chloroform to form a 1 wt % solution. The solution (50 μL) was coated onto a 24 mm × 24 mm cover slide (treated with 2% dimethyl dichlorosilane (Fluka)/chloroform solution in order to improve the contact angle and make the copolymer attach the cover slide more easily, then dried at 180 °C for 4 h before use) and then the solvent was removed by drying in the air for 30 min and following drying in vacuum for 12 h at room temperature. The cover slides were sterilized under UV radiation for 30 min. Rat C6 glioma cells were used to investigate the cell adhesion and viability of the several materials. The cells were rinsed three times with 0.1 M PBS by centrifugation at 1000 rpm for 5 min and cultured in cell culture flasks in a density of 2.0×10^4/cm^2 with RPMI 1640 medium (GIBCO) supplemented with 10% fetal calf serum (Gibco), 1.0×10^5/L penicillin (Sigma), and 100 mg/L streptomycin (Sigma), in a humidified incubator at 37 °C and 5% CO_2. The medium was changed every 2 days. After 3–5 days culture, the monolayer C6 cells were removed from the cell culture flasks by trypsin (0.25%) treatment and rinsed three times with 0.1 M PBS by centrifugation at 1000 rpm for 5 min. The obtained C6 cells were resuspended in the medium to adjust cell density to 1.0×10^5 cells/well (in 1 mL of medium), then seeded on the cover slides coated with the PLA, LM PLAAP, EM PLAAP, and EM PLAAP doped with CSA and a cover slide, which were placed into 6-well plates (Costar) and tissue-culture-treated polystyrene (TCPS) (the empty 6-well plates) before being sterilized under UV radiation for 30 min and washed three times with PBS. Then 3 mL of medium were added into each well to prevent the cover slide from floating during cell seeding. The plates were incubated at 37 °C and 5% CO_2 for 3, 6, 9, and 24 h, respectively. The cover slides were washed three times with PBS and fixed with 3% glutaraldehyde in PBS at room temperature for 30 min, washed with distilled water, and dried in air. After some culture time, the cells were fixed with glutaraldehyde at room temperature and stained by DMSO solution with 2% FITC fluorescein (Sigma) for 10 min, then washed by PBS solution for three times. Cell attachment and proliferation were observed under the reverse microscope (TE2000U, Nikon). The fluorescence pictures were taken by Digital Camera DXM1200F (Nikon) and analyzed with "NIH Image J" software (>20 per sample). The data presented are the mean ± standard deviation (SD). Independent and replicated experiments were used to analyze the statistical variability of the data, with $p < 0.05$ being statistically significant.

MTT Experiment. Cytotoxicity of PLA, AP, and PLAAP materials were assayed using MTT assay. First, PLA, AP, and PLAAP powders were respectively put into RPMI 1640 medium (Gibco) supplemented with 10% fetal calf serum (Gibco) for 48 h at 37 °C to get their extract liquid with the concentration of 100, 50, 25, 12.5, 6.25, 3.125, and 1.5625 mg/mL, respectively. C6 cells were seeded in 96-well plates at a density of 12000 cells per well and medium changed after 24 h incubation. Then various concentrations of extract liquid were then added to the wells. After incubating for 24 h, 20 μL of MTT stock solution in PBS (5 mg/mL) was added into each well with a final concentration of 0.5 mg/mL MTT. The plate was then incubated at 37 °C in 5% CO_2 for 4 h. The medium was removed and 200 μL of DMSO was added to dissolve the formazan crystals. The optical density (OD) was measured at 492 nm by a microplate reader (Multiskan MK3, Thermo USA). Untreated cells were taken as control with 100% viability. The relative cell viability (%) compared to control cells was calculated by $[abs]_{sample}/[abs]_{control} \times 100$.

Electrical Stimulation on PC-12 Cells. To evaluate the influence of electroactive substrate on neuronal differentiation stimulated by the electrical signals, rat neuronal pheochromocytoma PC-12 cells were adopted because of their outstanding sensitization to electrical stimulation. PC-12 cells were maintained in a humidified incubator and grown in Dulbecco's modified Eagle's medium (DMEM) supplemented with 10% heat-inactivated horse serum (Gibco), 5% fetal bovine serum (Gibco), and passaged using 0.25% trypsin at 1:2 dilution every other day under standard conditions (37 °C, 5% CO_2). PC-12 cells were seeded on TCPS and the EM PLAAP (doped with CSA) films coated onto a 24 mm × 24 mm cover slide (treated with 2% dimethyl dichlorosilane (Fluka)/chloroform solution) at a density of 10000 cells/well and were allowed for differentiate in the presence of NGF (50 ng/mL). Before seeding, TCPS and cover slides coated with EM PLAAP (doped with CSA) were sterilized by exposure to UV radiation for 1 h. The electrical stimulation was carried on the Signal Generator (Suing TFG6030 DDS), and the signals were displayed and checked on the wave inspector (Rigol DS1022C digital oscilloscope). The square wave, frequency of 1 Hz, 5% duty cycle, and electrical potential of 0.1V was adopted in the experiment. The electrical potential was added directly on the surface of TCPS and EM PLAAP (doped with CSA) films, respectively, through two microwire platinum electrodes (the diameter was 0.5 mm). The two samples were respectively stimulated for 1 h every day. Another two samples of TCPS and EM PLAAP (doped with CSA) films were not exposed to electrical stimulation as the contrast ones. After being cultured for 4 days, the cells were fixed with glutaraldehyde at room temperature and stained by DMSO solution with 2% FITC fluorescein (Sigma) for 10 min, then washed by PBS solution for three times. The neurite morphology was assessed using microscopic techniques. The fluorescence pictures were taken by a digital camera DXM1200F (Nikon). The neurite length of PC-12 cells from the cell body to the farthest tip of extension was measured by imaging software "NIH Image J" (>20 per sample). The data presented are the mean ± standard deviation (SD). Independent and replicated

Scheme 1. Schematic synthesis route and structure of PLAAP copolymer

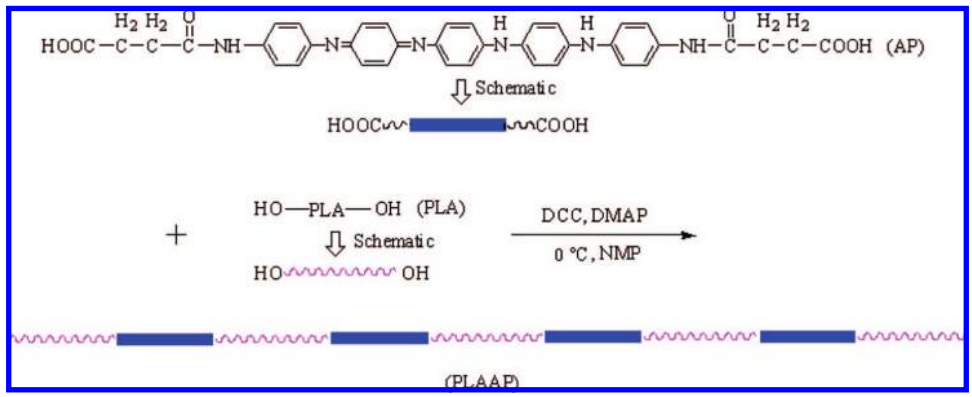

Table 1. Composition and GPC Data of the PLAAP Copolymer

samples	feed mol ratio[a]	mol wt of PLA[b]	wt fraction of EM AP (%)[c]	GPC of PLA			GPC of PLAAP copolymer		
				M_w	M_n	PDI	M_w	M_n	PDI
PLAAP	1:1	2.0k	25.2	2.14k	2.06k	1.04	89.8k	66.8k	1.34

[a] Ratio of PLA to EM AP unit. [b] Molecular weight of PLA, calculated from ^{1}H NMR. [c] Weight fraction of EM AP in the copolymers, calculated according to the molecular weight of PLA.

experiments were used to analyze the statistical variability of the data, with $p < 0.05$ being statistically significant.

3. Results and Discussion

3.1. Synthesis of PLAAP Copolymer. The vivid synthesis approaches were described in the preceding section. In brief, as the precursors, hydroxyl-capped poly(L-lactide) (PLA) and carboxyl-capped aniline pentamer (AP) were obtained according to the previous methods.[41] Then the condensation polymerization of PLA and AP with the feed molecular ratio of 1:1 was carried out in the concentrated NMP solution with DCC as the condensating agent and DMAP as the catalyst. The hydroxyls and carboxyls on both ends of PLA and AP, respectively, were combined with each other with ester bonds to form the long and multiblock PLAAP copolymer chain as shown in the Scheme 1. This soft−rigid alternative structure of PLAAP copolymer has two kinds of advantages: on one hand, the soft−rigid alternative structure is favored for the formation of phase separation that will lead to the improvement of the copolymer material's electrical conductivity; on the other hand, the degradation behavior can happen at the sites of every soft PLA segment in copolymer main chain, so this soft−rigid alternative structure is propitious to improve the degradation rate of copolymer materials. The key factor in this condensation polymerization is the control of reaction concentration and feed molecular rate of reactants. It is well-known that the efficiency of the condensation polymerization is correspondingly low. Only when the reaction concentration is very high and the reactants have the same mole ratio do the reactants have enough chances to meet each other and have equal activity in the competition reaction and then the condensation polymerization efficiency could be sufficiently ensured.

Table 1 shows the results of PLAAP copolymer composition, the molecular weight from proton nuclear magnetic resonance (^{1}H NMR), and gel permeation chromatography (GPC). The molecular weight of PLA determined from ^{1}H NMR was used in the calculation of reactant feed ratios in the synthesis of block copolymer. The molecular weight contrast of PLA and PLAAP copolymer according to GPC proved the successful synthesis of multiblock PLAAP copolymer. PLA with the molecular weight 2000 (determined from ^{1}H NMR) was selected as the optimum soft segment. This is because choosing a longer PLA chain will decrease the fraction of EM AP in copolymer, resulting in the decreasing of conductivity of copolymer, and choosing a shorter PLA chain will make against synthesizing high molecular weight copolymer with good mechanical properties.

The ^{1}H NMR spectrum was used to further demonstrate the structure of PLAAP copolymer. To avoid the complicated quinoid signals of emeraldine PLAAP (EM PLAAP) copolymer, Figure 1 shows the ^{1}H NMR (400 MHz, DMSO-d_6) spectrum of the fully reduced leucoemeraldine PLAAP (LM PLAAP) copolymer. The proton peaks of LM PLAAP copolymer were labeled at their corresponding positions in the ^{1}H NMR spectrum. The area of proton peak in $-CH_2-$ group (corresponding to the "f" proton in Figure 1) was almost the same with the one in phenyl (corresponding to the "2" proton in Figure 1), which demonstrated that the molecular ratio of hydroxyl-capped polylactide (PLA) segment and carboxyl-capped aniline pentamer (AP) segment was 1:1. This result further confirmed the alternatr multiblock structure of the PLAAP copolymer.

3.2. Electrochemical Characterization of PLAAP Copolymer. It is well-known that aniline oligomers such as polyaniline have different oxidation states when they are treated by different voltages or oxidant and reducer. Likewise, the PLAAP has three oxidation states, with the redox changes of AP segments similar to the PAP triblock copolymer described in our previous paper,[41] that is, leucoemeraldine state (LM), emeraldine state (EM), and pernigraniline state (PN). LM PLAAP copolymer had five benezene ring units in one AP segment. When the copolymer was in the EM state, there were four benezene ring units and one quinoid ring in one AP segment. Whereas, in the PN state of PLAAP copolymer, there were three benezene ring units and two quinoid ring units in one AP segment. The three oxidation states can repeatedly transform each other. The cyclic voltammogram spetrum was one of the best ways to illustrate the transitions between three oxdidation states shown in Figure 2. The first pair of redox peaks with the redox potential at 0.34 V correspond to the transition between the LM state and the EM state, and the second pair of peaks with the redox potential at

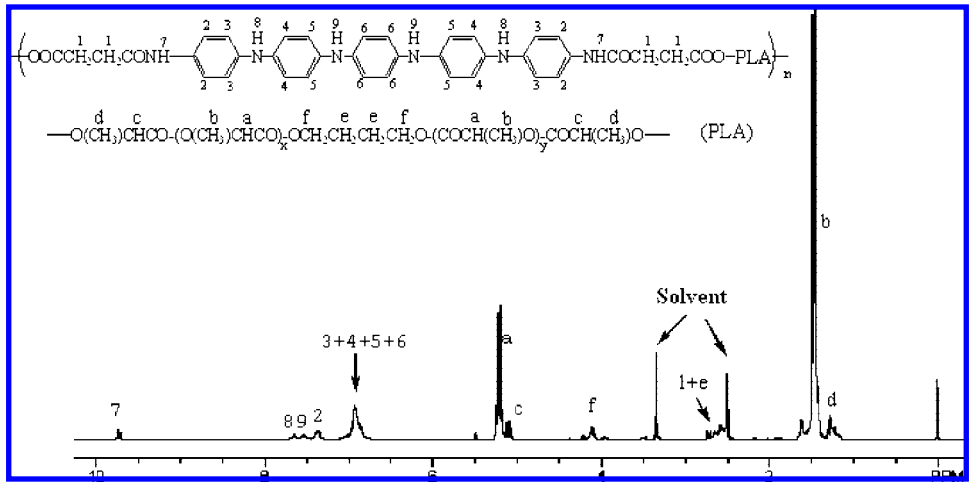

Figure 1. ^{1}H NMR spectrum (400 MHz, DMSO-d_6) of LM PLAAP copolymer in respective regions.

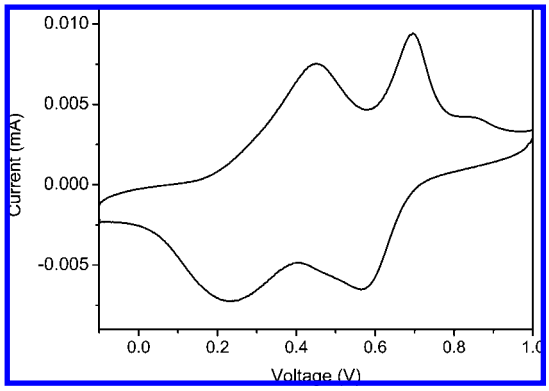

Figure 2. Cyclic voltamogram of PLAAP copolymer films on ITO glass in 1.0 M HCl using Ag/Ag$^+$ as reference electrode.

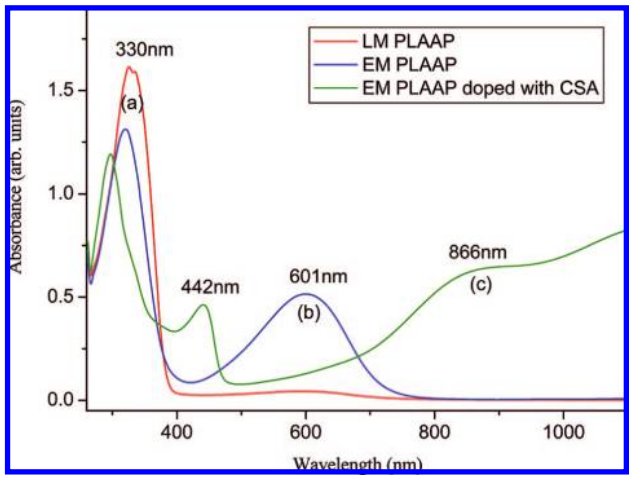

Figure 3. UV–visible spectra of PLAAP copolymer in DMF in LM state (a), EM state (b), and (c) EM state doped with camphorsulfonic acid (CSA).

0.63 V correspond to the transition between the EM state and the PN state. The transitions of three oxidation states to each other identified the good electroactivity of PLAAP copolymer.

Figure 3 shows the UV–visible spectra of PLAAP copolymer in DMF solution at different oxidation states. The only absorption peak at ~330 nm in Figure 3a represents the benzenoid peak arising from $\pi-\pi^*$ transition in the benzene unit of the AP segment in LM PLAAP copolymer. In EM PLAAP copolymer, besides the absorption peak at ~330 nm, the appearance of the new absorption peak at ~601 nm should be attributed to transition $\pi b-\pi q$ from benezene ring to quinoid ring. Figure 3c displays the characteristic absorbance spectra of EM PLAAP copolymer doped with camphorsulfonic acid (CSA). During the doping process, the color of solution changed from blue to green. The peaks at ~442 nm represent the polaron band, and the localized polaron peak at ~866 nm confirms the generation of emeraldine salts and the ability of conducting electrons of PLAAP copolymer. It is worthy of notice that the peak band (>1000 nm) shows a sharply upward trend. According to the theory of Xia et al.,[44] the absorption peak at ~866 nm is consistent with a coil-like conformation with shorter conjugation length and the absorption band in the near-infrared region is consistent with an expanded coil-like conformation and a delocalized polaron structure with larger conjugation length. Thus, the EM PLAAP copolymer doped with CSA should exhibit the better ability of conducting electrons with the larger conjugation length than PAP copolymer doped with CSA reported in our previous paper. In agreement with the theory prediction, the electric conductivity of EM PLAAP copolymer doped with CSA measured by experiment was $10^{-5}-10^{-6}$ S/cm, which is better than the one of PAP triblock copolymer doped with CSA.

3.3. Solubility and Surface Hydrophilicity. The solubility is one of the important factors to the processibility of materials in the practical application. PANi and aniline oligomers can only dissolved in a strong polar solution with high boiling point, including DMF, NMP, and DMSO, which lead to the increase of machining difficulty and cost of products. However, the PLAAP copolymer can dissolve in most of the common organic solutions such as $CHCl_3$ and THF due to the introduction of soluble PLA segments. The excellent solubility of PLAAP copolymer made the reprocessing of products convenient and low cost.

The surface hydrophilicity of the PLAAP copolymer films with different oxidation states and obtained from different solvents, as characterized by static water contact angle, is reported in Table 2. Obtained from the same solvents of $CHCl_3$, the contact angle of EM PLAAP decreased little compared to that of LM PLAAP, that is, because the hydrophilicity of AP segment in EM state was little higher than in the LM state. The solubility of AP segment of PLAAP copolymer varies in different solvents, so the surface conformation of PLAAP copolymer film may be correspondingly different and then influence the surface hydrophilicity of PLAAP film. In fact, whether EM PLAAP was dissolved in $CHCl_3$, THF, or DMF,

Table 2. Contact Angles of LM PLAAP and EM PLAAP Copolymer Thin Film from Different Solvents

samples	contact angles (deg)
LM PLAAP dissolved in $CHCl_3$	98 ± 2
EM PLAAP dissolved in $CHCl_3$	92 ± 1
EM PLAAP dissolved in THF	90 ± 2
EM PLAAP dissolved in DMF	89 ± 2
EM PLAAP dissolved in $CHCl_3$ doped with CSA	55 ± 3

their contact angles were approximately the same. This indicated that the surface hydrophilicity of PLAAP copolymer was not influenced by the solvent during the preparation of the copolymer films. When the EM PLAAP copolymer was doped with CSA, the hydrophilicity of EM AP segment greatly increased due to the form of salt and the contact angle decreased to about 55°.

3.4. Thermal Properties of PLAAP. Figure 4 represents the DSC thermograms of AP, PLA, and PLAAP powders. AP showed no glass-transition temperature (T_g) as an oligomer. The T_g of PLA was low at 23.1 °C due to the low molecular weight of ~2000. For PLAAP copolymer, the T_g increased much to 61.9 °C, which should be attributed to the introduction of hard AP segments in the PLAAP copolymer main chain. T_g is normally the highest temperature of the polymer used as the plastic with some rigidity. PLAAP copolymer can be processed into film or scaffold applied in vivo with enough mechanical strength due to the higher T_g than body temperature. So the T_g increase of PLAAP copolymer provided advantageous condition for the application as the scaffold materials in tissue engineering.

The TGA curve of the PLAAP copolymer by heating the sample from room temperature to 800 °C is displayed in Figure 5. The copolymer had a clear two-step decomposition path. The first weight loss step occurred in the temperature range 150–400 °C with a mass loss of about 80%, which could be attributed to the elimination of bounded dopant and the decomposition of PLA and BDO main chains. The subsequent loss step in the temperature range of 400–800 °C with a mass loss of about 14% should be due to the decomposition of BDO-unprotected aniline pentamer bone chain, which was just accordant with the proportion of the BDO-unprotected aniline pentamer in the

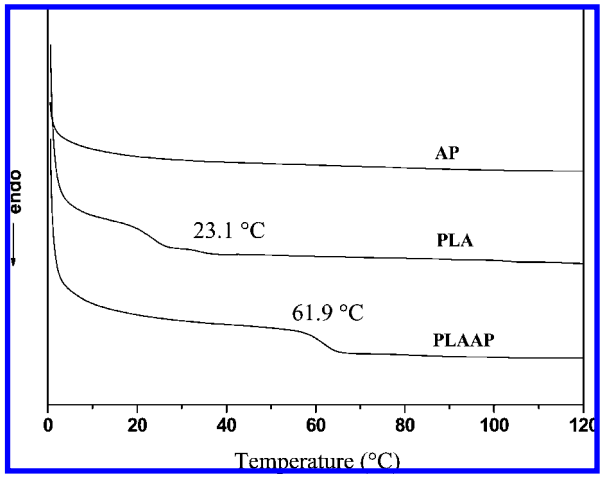

Figure 4. DSC heating curves of AP, PLA, and PLAAP (second heating).

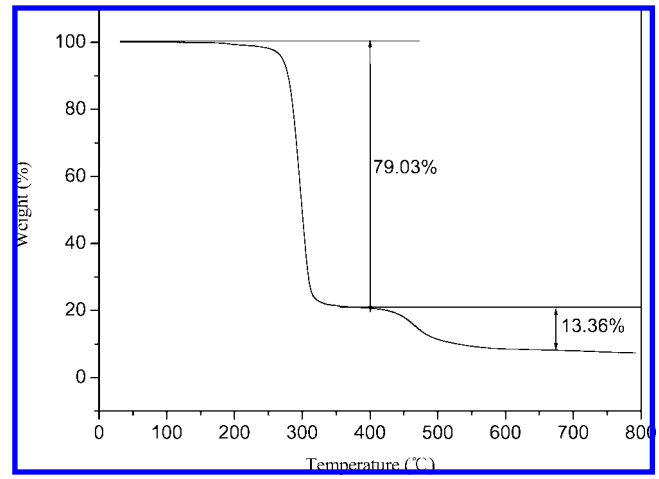

Figure 5. TGA thermogram of the PLAAP copolymer in N_2.

Table 3. Mechanical Properties of PLAAP Copolymer

sample	tensile strength (MPa)	tensile Young's modulus (MPa)	breaking elongation rate (%)
PLAAP copolymer	3.0	33	95

PLAAP copolymer. The rest mass loss of 6% was due to the carbonization of the copolymer. In fact, the obvious weight loss began from ~230 °C and the loss weight loss before 230 °C should be ascribed to the volatilization or decomposition of moisture and low-molecular-weight dopants, which indicates the pretty good thermal stability of PLAAP copolymer.

3.5. Mechanical Properties. Table 3 exhibits the mechanical properties of PLAAP copolymer. The PLAAP copolymer was highly distensible with tensile strength of 3.0 MPa and breaking elongation rate of 95% due to the alternate soft−rigid structure of the PLAAP copolymer chain. The tensile Young's modulus of PLAAP copolymer was not very high because the molecular weight of the soft segment PLA was comparatively low and PLA was amorphous, resulting in the intermolecular interaction that was comparatively weak.

3.6. In Vitro Biodegradation of PLAAP Copolymer Thin Films. The in vitro degradation of PLAAP copolymer film in Tris-HCl buffer solution containing proteinase K at 37 °C is shown in Figure 6. Environment conditions in vivo were simulated by Tris-HCl buffer solution containing proteinase K under 37 °C. The transparent degradation solution surrounding in PLAAP film appeared light blue after degradation for 24 h, and the color of the degradation solution changed to dark blue after degradation for 200 h. PLAAP copolymer showed a very fast degradation rate (60% weight loss at 200 h), which was a little slower than PLA with similar M_w (60% weight loss at 120 h). The difference was mainly caused by the seal of the end hydroxyl group in the PLA molecule, which plays an important role in degradation of PLA according to past reports.[45] The good biodegradability of PLAAP copolymer provided the antecedent condition of application in vivo.

3.7. Cytotoxicity Assessment of Degradation Products. The PLAAP copolymer was designed to generate two nontoxic degradation products after hydrolytic cleavage: low-molecular-weight block copolymer and lactic acid oligomers. The lactic acid oligomers are well-known for nontoxicity. The low-molecular-weight block copolymer was proved to be innocuous and biocompatible in our previous paper.[41] To determine the cytotoxicity of the PLAAP copolymer in comparison with PLA

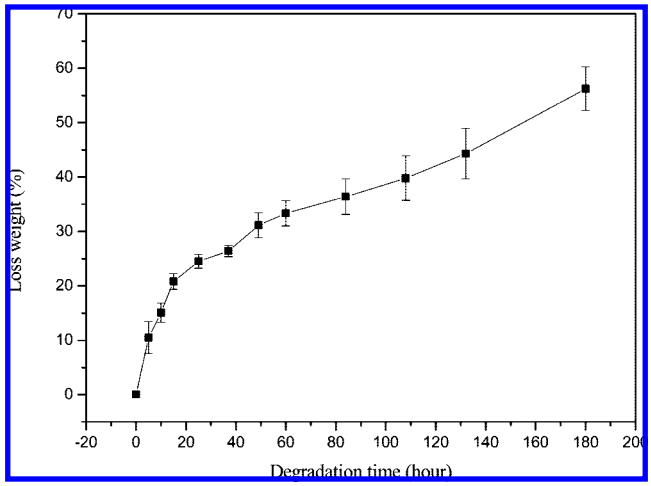

Figure 6. Degradation of the PLAAP copolymer. Degradation studies of PLAAP films (10 mm × 10 mm × 0.2 mm) were performed in Tris-HCl buffer containing proteinase K (pH = 8.6) at 37 °C.

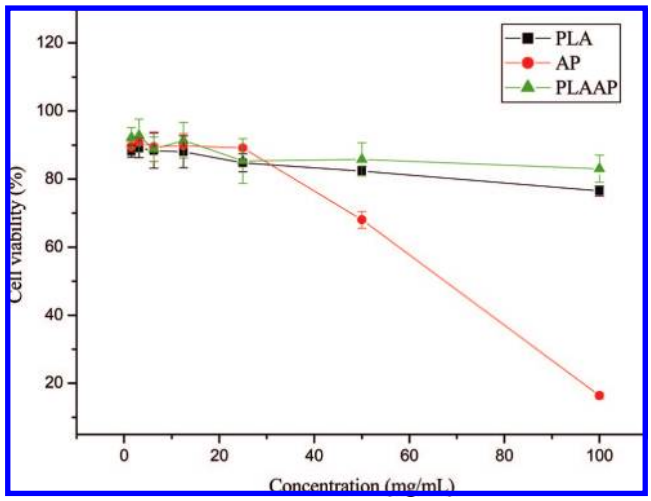

Figure 7. Cytotoxicity of AP, PLA, and PLAAP in vitro. Viability of rat C6 cells is expressed as a function of polymer concentration.

and AP, the MTT assay by the rat C6 cell line is shown in Figure 7. Cells were incubated with the increasing elution solution concentration of PLA, AP, and PLAAP ranging from 1.65 to 100 mg/mL as described in the Experimental Section. As expected, the cell viability rate of PLAAP copolymer was very high in each concentration similar to PLA, the nontoxic positive reference. Pure AP exhibited low cell viability compared to that of PLA and PLAAP, which indicated that the successful improvement of AP cytotoxicity through the copolymerization with PLA.

3.8. In Vitro Biocompatibility Assessment of PLAAP Copolymer. To deeply evaluate the biocompatibility of PLAAP copolymer in vitro, six kinds of material were prepared to contrast. They were: controlled tissue-culture-treated polystyrene (TCPS), silane-treated cover-slide (glass), PLA, LM PLAAP, EM PLAAP, and EM PLAAP doped with CSA. C6 cells were seeded on them and cultured for 3, 6, 9, and 24 h, respectively, to observe the cell adhesion and proliferation. The area fraction occupied by the adhering cells on the polymer film was counted by NIH Image J. Figure 8 gives the area fraction histogram of six materials cultured for different time. Cultured for 3 h, TCPS showed excellent adhesion ability, while the adhesion of PLA was comparatively bad. The adhesion abilities of the other four materials were appropriately the same between TCPS and PLA.

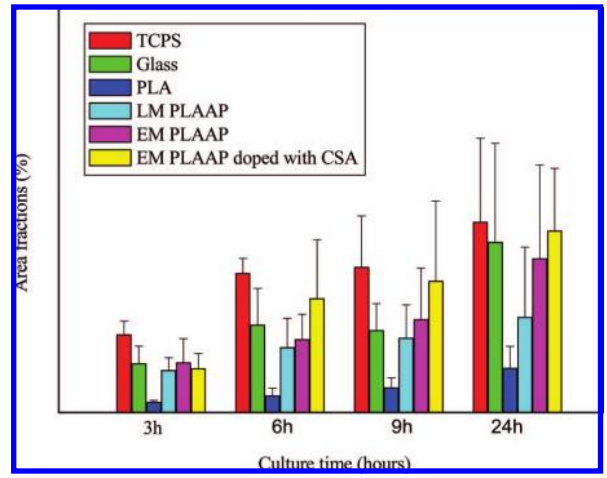

Figure 8. Area fraction of the C6 cells adhered and proliferated on the surface of the TCPS, glass, PLA, LM PLAAP, EM PLAAP, and EM PLAAP doped with CSA at various time points. Results represent mean ± SD from three separate experiments ($P < 0.05$).

Along with culture time increasing from 6 to 24 h, the adhesion and proliferation of EM PLAAP doped with CSA showed dramatic improvement, especially, the cell area fraction of EM PLAAP was higher than that of TCPS cultured for 24 h. PLA remained a bad adhesion and proliferation compared to other materials. The area fraction of glass was almost parallel to EM PLAAP and a little higher than LM PLAAP. It was reported that the cell adhesion and proliferation ability of materials could be influenced by the surface hydrophilicity of materials.[27] Studies have shown that contact angles in the range of 40−70° maximize the adhesion of multiple cell types.[30] The contact angle of PLA measured was 115°, so it showed bad cell adhesion. The contact angle of LM PLAAP was about 98° (shown in Table 2), and its adhesion ability improved compared to that of PLA. The contact angle of EM PLAAP was about 92° (shown in Table 2) like glass (treated by silane), and so they exhibited the similar cell area fraction. The contact angle of EM PLAAP doped with CSA decreased to about 55°, which was in the suitable range of cell adhesion, so it showed good adhesion and proliferation ability similar to TCPS, the good biocompatible surface coated with special bioactive materials.

Figure 9 shows the average area (the mean size of the adhering cells on polymer film shown in the images) of C6 cells in cover slide coated with six different materials, respectively (similar to the materials in Figure 8), analyzed by NIH Image J software. After being cultured for 3 h, the cell average areas of six materials were almost the same. With the increase of culture time, the cell average areas of different materials differentiated distinctly. Especially for 24 h, the cell average area of PLA was smallest, and the cell average area of LM PLAAP, EM PLAAP, and glass similar to TCPS increased in order and then EM PLAAP doped with CSA was the biggest, which even exceeded TCPS. The cell average area was related to the surface characterization of materials on one hand, and on the other hand, the important electroactivity effect of PLAAP copolymer may accelerate the growth of C6 cells. Particularly, EM PLAAP doped with CSA could be easy to display its electroactivity in PBS buffer and benefit the chemical and energy exchange between cells and surrounding, then accelerate the growth of cells.

3.9. Influence on Differentiation of PC-12 Cells Stimulated by Electrical Signal. It has been proved that the electroactive polymers can promote the neuronal differentiation

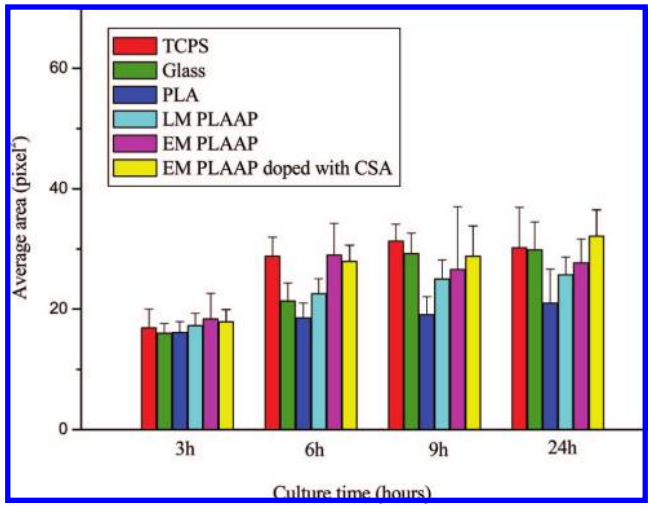

Figure 9. Average area of the C6 cells adhered and proliferated on the surface of the TCPS, glass, PLA, LM PLAAP, EM PLAAP, and EM PLAAP doped with CSA at various time points. Results represent mean ± SD from three separate experiments ($P < 0.05$).

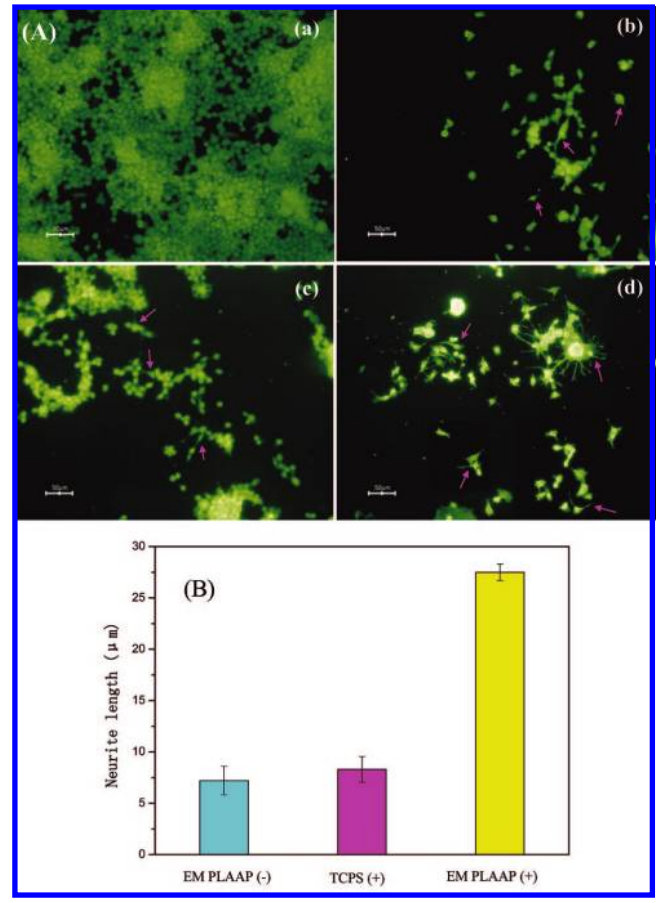

Figure 10. (A) Representational fluorescence micrographs of PC-12 cell for the substrates (a) TCPS (−) (TCPS without electrical stimulation), (b) TCPS (+) (TCPS exposed to electrical stimulation), (c) EM PLAAP (−) (EM PLAAP doped with CSA without electrical stimulation), (d) EM PLAAP (+) (EM PLAAP doped with CSA exposed to electrical stimulation) on day 4. (B) The mean neurite length of PC-12 cells cultured on the substrates of EM PLAAP (−), TCPS (+), and EM PLAAP (+) on day 4. Date are expressed as mean ± SD from three separate experiments ($P < 0.05$).

stimulated by the electrical signals, just as mentioned previously. For PLAAP copolymer, our ultimate goal was realizing the practical application as the scaffold materials in neural tissue engineering and accelerating nerve repair. Rat neuronal pheochromocytoma PC-12 cells are sensitive to electrical stimulation and easy to express their phenotype. We expected that the electroactive PLAAP copolymer could promote the differentiation of PC-12 cells stimulated by electrical signals. During the functional differentiation process, PC-12 cells gradually extended from the original circular shape to the neuronal phenotype. As shown in Figure 10A, seeded on the EM PLAAP doped with CSA on day 4, only a few PC-12 cells expressed the trend of neurite extension when the cells were not stimulated by electrical signals (Figure 10A(c)), however, exposed to electrical stimulation, most of PC-12 cells showed the neurite extension and some of them grew out of the clear "neural networks" in particular (Figure 10A(d)). Compared to PC-12 cells on the TCPS surface, whether exposed to electrical stimulation or not (Figure 10A(a) and (b)), the trends of neurite extension were not obvious, especially, PC-12 cells on TCPS without stimulation had not differentiated basically. Only a few PC-12 cells expressed the neurite extension seeded on TCPS stimulated by electrical signals, and obviously, the cell conglomeration phenomena were solved through electrical stimulation whether on TCPS or electroactive copolymer surface, which provided the conditions for neurite extension. The effect of electrical stimulation on electroactive material surface may be the acceleration of interaction between materials and cells by changing the electroactive materials' surface properties. The conclusion from the micrographs could be confirmed by the mean neurite length of PC-12 cells on different substrates shown in Figure 10B. Accordant with the information observed from micrographs, the mean neurite length of PC-12 cells on EM PLAAP exposed to electrical stimulation were 27.5 ± 0.8 μm, much higher than TCPS exposed to electrical stimulation and EM PLAAP without stimulation. These results above indicate that the electroactive PLAAP surface could indeed accelerate the differentiation of nerve cells stimulated by electrical signals as expected.

4. Conclusions

Designing the stimulus−response and specially functionalized polymers as bioactive materials is one of the important developing orientations of biomaterials. Novel biomaterials should be highly critical in providing the optimal environment favor for the growth of cells and the elaboration of function in vitro. So, we synthesized one multiblock copolymer PLAAP via the condensation reaction of PLA and AP blocks. This PLAAP copolymer had excellent electroactivity similar to polyaniline and AP, which provided the special function to improve the adhesion, growth, and proliferation of cells. Because of the PLA segments in PLAAP main chains, the copolymer was biodegradable, which solved the application problem of conducting or electroactive polymers in vivo for a long time. Moreover, the PLAAP copolymer showed good solubility and mechanical properties, so it was easy to process the copolymer material in practical application. In vitro cell experiments proved that the PLAAP substrate was biocompatible and a help for the differentiation of nerve cells. The PLAAP copolymer successfully achieved the goal as a novel functionalized biomaterial and a good candidate for the electroactive polymers used in biomedical field. Future work will focus on designing the appropriate electroactive dimensional scaffold model and evaluating the tissue compatibility through the animal test in vivo.

Acknowledgment. Financial support was provided by the National Fund for the Distinguished Young Scholars (no. 50425309) and by the National Natural Science Foundation of

China (no. 50773081, Key Program no. 50733003), and Y. Wei is most grateful to the Chinese Academy of Sciences for an Outstanding Overseas Scholar Award.

References and Notes

(1) Langer, R.; Cima, L. G.; Tamada, J. A.; Wintermantel, E. *Biomaterials* **1990**, *11*, 738–745.
(2) Dietmar, W. H. *Biomaterials* **2000**, *21*, 2529–2543.
(3) Lakshimi, S. N.; Cato, T. L. *Prog. Polym. Sci.* **2007**, *32*, 762–798.
(4) Gentleman, E.; Lay, A. N.; Dickerson, D. A. *Biomaterials* **2003**, *24*, 3805–3813.
(5) Madihally, S. V.; Matthew, H. W. T. *Biomaterials* **1999**, *20*, 1133–1142.
(6) Nakamatsu, J.; Torres, F. G.; Troncoso, O. P.; Min-Lin, Y.; Boccaccini, A. R. *Biomacromolecules* **2006**, *7*, 3345–3355.
(7) Gugala, Z.; Gogolewski, S. *J. Biomed. Mater. Res.* **2000**, *49*, 183–191.
(8) Schugens, Ch.; Maquet, V.; Grandfils, Ch.; Jerome, R.; Teyssie, Ph. *J. Biomed. Mater. Res.* **1996**, *30*, 449–461.
(9) Cai, Q.; Wan, Y.; Bei, J.; Wang, S. *Biomaterials* **2003**, *24*, 3555–3562.
(10) Li, W.; Danielson, K. G.; Alexander, P. G.; Tuan, R. S. *J. Biomed. Mater. Res.* **2003**, *67*, 1105–1114.
(11) Ma, L.; Gao, C.; Mao, Z.; Zhou, J.; Shen, J.; Hu, X.; Han, C. *Biomaterials* **2003**, *24*, 4833–4841.
(12) Zhao, J.; Yuan, X.; Cui, Y.; Ge, Q.; Yao, K. *J. Appl. Polym. Sci.* **2004**, *91*, 676–1684.
(13) Zhang, Y. Z.; Venugopal, J.; Huang, Z.-M.; Lim, C. T.; Ramakrishna, S. *Biomacromolecules* **2005**, *6*, 2583–2589.
(14) Lee, C.; Huang, C.; Lee, Y. *Biomacromolecules* **2006**, *7*, 2200–2209.
(15) Willner, I.; Rubin, S. *Angew. Chem., Int. Ed. Engl.* **1996**, *35*, 367–385.
(16) George, P. M.; LaVan, D. A.; Burdick, J. A.; Chen, C.; Liang, E.; Langer, R. *Adv. Mater.* **2006**, *18*, 577–581.
(17) Kim, B.; Qiu, J.; Wang, J.; Taton, T. A. *Nano Lett.* **2005**, *5*, 1987–1991.
(18) Jones, M. C.; Ranger, M.; Leroux, J. C. *Bioconjugate Chem.* **2003**, *14*, 774–781.
(19) Millesi, H. *Operative Nerve Repair and Reconstruction*; Gelberman, R. H., Ed.; Lippincott: Philadelphia, 1991, pp 525–544..
(20) Sisken, B. F.; Kanje, M.; Lundborg, G.; Herbst, E.; Kurtz, W. *Brain Res.* **1989**, *485*, 309–316.
(21) Kens, J. M.; Fakhouri, A. J.; Weinrib, H. P.; Freeman, J. A. *Neuroscience* **1991**, *40*, 93–107.
(22) Basser, P. *J. Biomed. Eng.* **1994**, *41*, 601–606.
(23) MacDiarmid, A. G.; Chiang, J. C.; Richter, A. F.; Epstein, A. J. *Synth. Met.* **1987**, *18*, 285–290.
(24) Kanatzidis, M. G. *Chem. Eng. News* **1990**, *68*, 36–54.
(25) Iseki, M.; Saito, K.; Kuhara, K.; Mizukami, A. *Synth. Met.* **1991**, *40*, 117–126.
(26) Barngrover, D. *Mammalian Cell Technology*; Thilly, W. G., Eds.; Butterworths: Boston, 1986; pp 131–150..
(27) Wong, J. Y.; Langer, R.; Ingber, D. E. *Proc. Natl. Acad. Sci. U.S.A.* **1994**, *91*, 3201–3204.
(28) Kotwal, A.; Schmidt, C. E. *Biomaterials* **2001**, *22*, 1055–1064.
(29) Schmidt, C. E.; Shastri, V. R.; Vacanti, J. P.; Langer, R. *Proc. Natl. Acad. Sci. U.S.A.* **1997**, *94*, 8948–8953.
(30) Rivers, T. J.; Hudson, T. W.; Schmidt, C. E. *Adv. Funct. Mater.* **2002**, *12*, 33–37.
(31) Lakard, S.; Herlem, G.; Valles-Villareal, N.; Michel, G.; Propper, A.; Gharbi, T.; Fahys, B. *Biosens. Bioelectron.* **2005**, *20*, 1946–1954.
(32) George, P. M.; Lyckman, A. W.; LaVan, D. A.; Hegde, A.; Leung, Y.; Avasare, R.; Testa, C.; Alexander, P. M.; Langer, R.; Sur, M. *Biomaterials* **2005**, *26*, 3511–3519.
(33) Wan, Y.; Wu, H.; Wen, D. *Macromol. Biosci.* **2004**, *4*, 882–890.
(34) Castano, H.; O'Rear, E. A.; McFetridge, P. S.; Sikavitsas, V. I. *Macromol. Biosci.* **2004**, *4*, 785–794.
(35) Jiang, X.; Marois, Y.; Traore, A.; Tessier, D.; Dao, L. H.; Guidoin, R.; Zhang, Z. *Tissue Eng.* **2002**, *8*, 635–647.
(36) Mattioli-Belmonte, M.; Giavaresi, G.; Biagini, G.; Virgili, L.; Giacomini, M.; Fini, M.; Giantomassi, F.; Natali, D.; Torricelli, P.; Giadino, R. *Int. J. Artif. Organs* **2003**, *26*, 1077–1085.
(37) Wei, Y.; Lelkes, P. I.; MacDiarmid, A. G.; Guterman, E.; Cheng, S.; Palouian, K.; Bidez, P. In *Contemporary Topics in Advanced Polymer Science and Technology*; Peking University Press: Beijing, 2004; 430−436.
(38) Guterman, E.; Cheng, S.; Palouian, K.; Bidez, P.; Lelkes, P. I.; Wei, Y. *Polym. Prepr.* **2002**, *43*, 766–767.
(39) Bidez, P.; Li, S.; MacDiarmid, A. G.; Venancio, E. C.; Wei, Y.; Lelkes, P. I. *J. Biomater. Sci., Polym. Ed.* **2006**, *17*, 199–212.
(40) Li, M.; Guo, Y.; Wei, Y.; MacDiarmid, A. G.; Lelkes, P. I. *Biomaterials* **2006**, *27*, 2705–2715.
(41) Huang, L.; Hu, J.; Lang, L.; Wang, X.; Zhang, P.; Jing, X.; Wang, X.; Chen, X.; Lelkes, P. I.; MacDiarmid, A. G.; Wei, Y. *Biomaterials* **2007**, *28*, 1741–1751.
(42) Putnam, D.; Langer, R. *Macromolecules* **1999**, *32*, 3658–3662.
(43) Wang, Z. Y.; Yang, C.; Gao, J. P.; Lin, J.; Meng, X. S. *Macromolecules* **1998**, *31*, 2702–2704.
(44) Xia, Y.; MacDiamid, A. G.; Epstein, A. J. *Macromolecules* **1994**, *27*, 7212–7214.
(45) Riva, R.; Schmeits, S.; Stoffelbach, F.; Jerome, C.; Jerome, R.; Lecomte, P. *Chem. Commun* **2005**, 5334–5336.

BM7011828